Citation: Cell Death and Disease (2012) 3, e385; doi:10.1038/cddis.2012.113

www.nature.com/cddis

Leishmania mexicana metacaspase is a negative regulator of amastigote proliferation in mammalian cells

E Castanys-Muñoz[1], E Brown[1], GH Coombs[2] and JC Mottram*[,1]

Metacaspases (MCAs) are caspase family cysteine peptidases that have been implicated in cell death processes in plants, fungi and protozoa. MCAs have also been suggested to be involved in cell cycle control, differentiation and clearance of aggregates; they are virulence factors. Dissecting the function of MCAs has been complicated by the presence in many organisms of multiple *MCA* genes or limitations on genetic manipulation. We describe here the creation of a *MCA* gene-deletion mutant (Δ*mca*) in the protozoan parasite *Leishmania mexicana*, which has allowed us to dissect the role of the parasite's single *MCA* gene in cell growth and cell death. Δ*mca* parasites are viable as promastigotes, and differentiate normally to the amastigote form both in *in vitro* macrophages infection and in mice. Δ*mca* promastigotes respond to cell death inducers such as the drug miltefosine and H_2O_2 similarly to wild-type (WT) promastigotes, suggesting that MCAs do not have a caspase-like role in execution of *L. mexicana* cell death. Δ*mca* amastigotes replicated significantly faster than WT amastigotes in macrophages and in mice, but not as axenic culture *in vitro*. We propose that the *Leishmania* MCA acts as a negative regulator of amastigote proliferation, thereby acting to balance cell growth and cell death.

Cell Death and Disease (2012) **3,** e385; doi:10.1038/cddis.2012.113; published online 6 September 2012
Subject Category: Immunity

Apoptosis is a process of programmed cell death (PCD) required in multicellular organisms for normal tissue development and homoeostasis, as it eliminates cells that are damaged, infected or no longer needed.[1] A number of the biochemical and morphological events that define apoptosis have been described in the kinetoplastid parasites *Trypanosoma brucei* and *Leishmania*, which cause the important neglected tropical diseases African trypanosomiasis and leishmaniasis, respectively.[2] *Leishmania* has a digenetic life cycle, with two main morphological forms alternating between two hosts. Motile flagellated promastigotes proliferate as free-living cells in the sand fly.[3] They are transmitted by the bite of the sand fly and, once inside a mammalian host, they are taken up by phagocytes, where they transform into intracellular amastigotes. They multiply and the disease progresses due to further infection of macrophages with amastigotes.[4]

The apoptosis-like processes reported to occur in these kinetoplastid parasites include cell shrinkage, DNA fragmentation, activation of peptidases, mitochondrial depolarisation, release of cytochrome C, phosphatidylserine (PS) exposure and translocation of endonuclease G.[2,5] Such morphological and biochemical features have been described for different *Leishmania* species under a variety of stress stimuli, including nitric oxide or reactive oxygen species (ROS) produced by the host, hydrogen peroxide, heat shock, and the leishmanicidal drugs miltefosine (MLF) and camptothecin (CPT).[6–12] Current thinking proposes that unicellular parasitic protozoa such as *Leishmania* undergo apoptotic-like PCD as an altruistic trait to control parasite numbers to prolong survival of the host and parasite.[13] Although evolutionary theory can provide a framework to understand why unicellular organisms might undergo PCD, questions remain about the molecular mechanisms responsible for induction of such cell death. In particular, caspases, which have an essential role in the execution of apoptosis in higher eukaryotes, are absent from genomes of *Leishmania* and *Trypanosoma*.[14,15] Thus, it remains crucial to rigorously analyse possible cell death pathways and effector proteins regulating cell death in *Leishmania* and related protozoa to identify which cell death mechanisms are truly operating.

Metacaspases (MCAs) are cysteine peptidases grouped in clan CD, family 14. They are present in plants, yeast and protozoan parasites, but absent from mammals, and are distantly related to caspases, thus have been promoted to have caspase-like biological functions.[16] MCAs have a conserved caspase-like histidine–cysteine catalytic dyad, yet they have different substrate specificity from caspases and prefer arginine/lysine in the P1 position rather than the aspartic acid residue preferred by caspases.[17–19] MCAs are activated by calcium and autocatalytic processing has been

[1]Wellcome Trust Centre for Molecular Parasitology, Institute of Infection, Immunity and Inflammation, College of Medical, Veterinary and Life Sciences, University of Glasgow, Glasgow G12 8TA, UK and [2]Strathclyde Institute of Pharmacy and Biomedical Sciences, University of Strathclyde, Glasgow G4 0RE, UK
*Corresponding author: JC Mottram, Wellcome Trust Centre for Molecular Parasitology, University of Glasgow, 120 University Place, Glasgow G12 8TA, UK. Tel: +44 0 141 330 3745; Fax: +44 0 141 330 8269; E-mail: jeremy.mottram@glasgow.ac.uk
Keywords: metacaspase; caspase; cysteine peptidase; programmed cell death
Abbreviations: *BLE*, phleomycin-resistance gene; *HYG*, hygromycin-resistance gene; MCA, metacaspase; MLF, miltefosine; PCD, programmed cell death; PEMs, peritoneal exudate macrophages; TMRM, tetramethylrhodamine methyl ester perchlorate; TSN, Tudor staphylococcal nuclease; WT, wild type
Received 05.6.12; revised 06.7.12; accepted 06.7.12; Edited by A Stephanou

described for many MCAs, although this processing is not apparently necessary for enzymatic activity.[17,18,20] The structural basis for the substrate specificity and calcium activation has recently become apparent from the X-ray structure of the MCA2 from *T. brucei*.[21] Few natural substrates of MCAs are known, although the finding that Tudor staphylococcal nuclease (TSN), cleaved by the *Picea abies* MCA mcII-Pa during embryogenesis and induced PCD, is a substrate for both MCAs and caspases has been used as evidence of an evolutionary conserved cell death pathway in plants and animals.[22]

The report that the yeast MCA had a role in cell death[23] triggered a series of similar studies investigating such a role for other MCAs.[23] Subsequently, however, a number of other functions have been established for yeast MCA, from cell cycle involvement to clearance of insoluble aggregates.[24,25] In the plant *Arabidopsis thaliana*, MCAs have antagonistic influences on cell death – with AtMC1 promoting cell death, whereas AtMC2 inhibits it.[26] The single MCA of *Leishmania major* was described to have an important role in the cell cycle,[27] while it has also been reported to be involved in oxidative stress-induced cell death.[28] The MCA of *Leishmania donovani* has been proposed to have a role in cell death pathways[29,30] and also the cell cycle.[30]

The aim of this study was to provide additional insights into the role of MCA of *Leishmania* and related organisms by generating an *MCA*-deficient mutant. This achievement with *Leishmania mexicana* has allowed us to evaluate critically the possible participation of the single MCA in cell death and cell growth pathways. The data demonstrate that MCA is not essential for *Leishmania* survival or differentiation and, while not ruling out a role in regulated cell death, provide no evidence for such a role. In contrast, MCA clearly is implicated in the regulation of parasite replication inside the mammalian host.

Results

Generation of *L. mexicana MCA* null mutants. We were unsuccessful in our attempts in a previous study to generate *L. major MCA* gene deletion mutants and MCA overexpression lines had a severe growth defect, which we interpreted as being due to the importance of MCA levels to cellular replication.[27] To be able to analyse the role of MCAs more fully, we decided to investigate the protein of *L. mexicana*. *L. mexicana* is an excellent experimental model as it can be cultivated *in vitro* in both promastigote and amastigote-like life cycle stages and its virulence can be assessed both in macrophage infection studies *in vitro* and the formation of murine lesions *in vivo.* Having identified the *MCA* gene of *L. mexicana*, which encodes a predicted protein of 48 kDa that has 89% identity with *L. major* MCA, we used the Nucleofector, a newly developed system that provides high-efficiency transfection while being protective of cellular function, to genetically manipulate *MCAs* in *L. mexicana*. To our surprise, this improved transfection procedure allowed us to generate *MCA* null mutant cell lines (Δ*mca*; Figure 1a). Southern blot analysis confirmed the replacement of both *MCA* alleles, the 0.8-kb fragment detected in the wild type (WT) with a 5′ FR probe in an *Age*I/*Sac*II-digested genomic DNA being replaced in Δ*mca* parasites by 2.2- or 5-kb fragments corresponding to the hygromycin-resistance gene (*HYG*) or phleomycin-resistance gene (*BLE*) casettes, respectively (Figure 1b). A probe comprising 500 bp of the *MCA* open reading frame (ORF) was used to confirm the absence of the gene (Figure 1b, lower panel, lane 3). The absence of MCA was further confirmed by western blotting, using an affinity purified antibody raised against a peptide containing the C-terminal 15 amino acids of *L. major* MCA (designated αLmjMCA, 27; Figure 1c, lane 2, arrowed). *MCA* was reintroduced into the ribosomal locus, to give Δ*mca*::*MCA*. Re-expression of MCA was confirmed by western blot analysis, where MCA was detected at slightly higher levels of expression in the re-expressor cell line than in the WT promastigotes (Figure 1c, lane 3). The antibody recognised a number of cross-reacting proteins in Δ*mca*, but also processed products (lane 3). *L. mexicana* promastigotes overexpressing either MCA (designated WT (MCA)) or an active site mutant in which the two cysteines in the active site have been mutated to glycines (designated WT ($MCA^{C201-202G}$)) were also generated. Western blot analysis using the MCA antibody showed an increased level of the protein and the processed products in both WT (MCA) and WT ($MCA^{C201-202G}$) (Figure 1d, lanes 4 and 5) compared with WT, in which equivalent proteins cannot be visualised at this exposure (lane 1) and Δ*mca*::*MCA* (lane 3).

Slight variations in growth of the different lines of promastigotes were observed *in vitro*, Δ*mca*::*MCA* reached a higher density at day 6 than WT whereas WT ($MCA^{C201-202G}$) obtained a lower density than WT (Figure 1e). The DNA content of WT, Δ*mca*, WT (MCA) and Δ*mca*::*MCA* promastigotes was analysed by fluorescence-activated cell sorting (FACS); each had normal DNA content with two peaks corresponding to cells in G1 and G2/M (data not shown). In contrast to promastigotes, axenic amastigotes of Δ*mca* grew to a higher density than WT at day 9, whereas amastigotes of WT (MCA) had a markedly reduced growth rate compared with WT. Re-expression of MCAs in the Δ*mca*::*MCA* largely restored the growth of axenic amastigotes to WT levels (Figure 1f). To assess the subcellular location of *L. mexicana* MCA, the expression of MCAs in the different cell lines was analysed by immunofluorescence using αLmjMCA.[27] MCA was found to be mainly cytoplasmic, being present in punctate structures throughout the cell body in WT, WT (MCA) and Δ*mca*::*MCA*; its absence from Δ*mca* promastigotes served as a control (Figure 2).

MCA-deficient mutants are more virulent. The ability of the different lines to infect and multiply within peritoneal exudate macrophages (PEMs) was assessed. The percentage of infected PEMs with WT, Δ*mca* and Δ*mca*::*MCA* did not significantly differ at 3, 24 or 72 h. A small increase was observed at 120 h for Δ*mca*, most likely due to lysis of some heavily infected macrophages and infection of additional PEMs by the released amastigotes (Figure 3a). The intracellular proliferation, however, was greater for Δ*mca* than WT with there being significantly greater numbers of intracellular amastigotes at 72 and 120 h (Figure 3b). We also investigated whether overexpressing MCAs had any effect upon virulence in PEMs. The number of PEMs infected

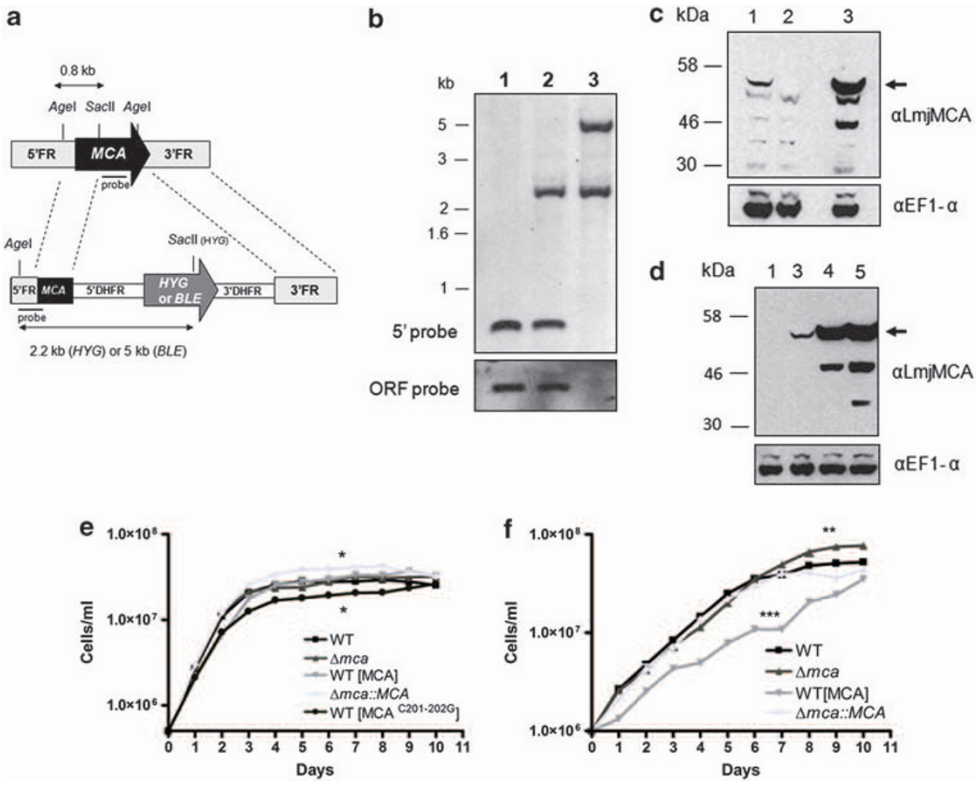

Figure 1 Generation of MCA null mutants. (**a**) Schematic representation of the *L. mexicana* WT *MCA* locus and the constructs used for targeted gene replacement. ORFs are shown as arrows, 5′FR plus 5′ end of *MCA*, and 3′FR DNA sequences used for gene targeting are shown as boxes. Restriction sites within the WT locus and the construct are shown, and the predicted sizes after DNA digestion are indicated for both native and modified *MCA* locus. *DHFR*, *dihydrofolate reductase gene*. (**b**) Southern blot analysis. Genomic DNA was digested with *Age*I/*Sac*I and hybridised with a labelled DNA probe comprising the 5′region used for gene targeting (upper) or an ORF probe (lower). Molecular mass markers are shown on the left. WT (lane 1), heterozygote (lane 2) and Δ*mca* (lane 3). (**c** and **d**) Western blot analysis. Whole-cell lysates of *L. mexicana* promastigotes were probed with anti-*L. major* MCA antibody. WT (lane 1), Δ*mca* (lane 2), Δ*mca*::*MCA* (lane 3), WT (MCA) (lane 4) and WT ($MCA^{C201-202G}$) (lane 5). EF1-α was used as a loading control. (**e**) Growth curve of *L. mexicana* promastigotes: WT (■), Δ*mca* (▲), Δ*mca*::*MCA* (◆), WT (MCA) (▼), WT ($MCA^{C201-202G}$)(●). (**f**) Growth curve of *L. mexicana* axenic amastigotes: WT (■), Δ*mca* (▲), Δ*mca*::*MCA* (◆), WT (MCA) (▼). ***, ** and * significant differences compared with WT (*t*-test, ***$P<0.001$, **$P<0.01$ and *$P<0.05$)

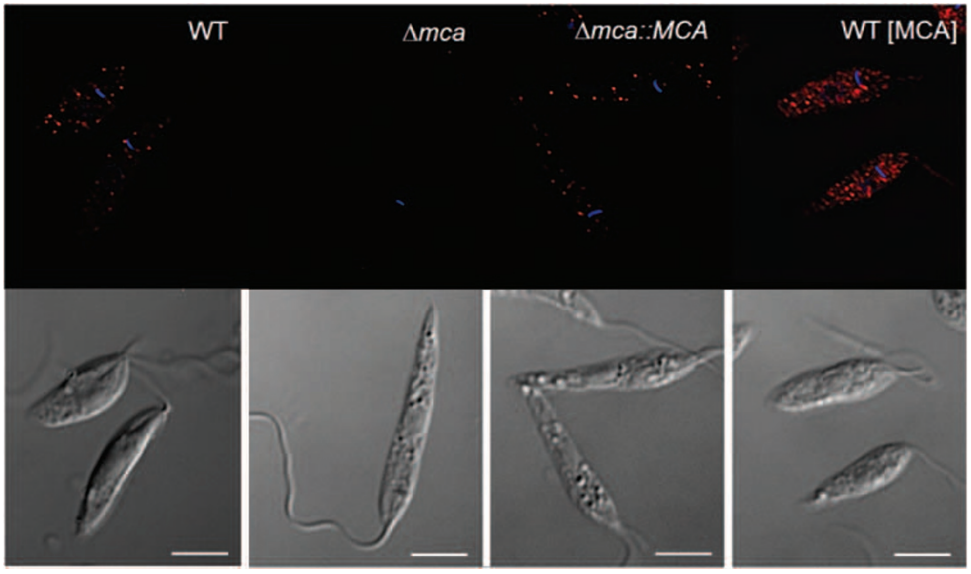

Figure 2 MCA localisation. Immunofluorescence analysis performed on *L. mexicana* promastigotes, using anti-LmjMCA antibody and Alexa fluor 594-conjugated anti-rabbit antibody (red). Upper panels, immunofluorescence on cell lines as indicated. Lower panels, differential interference contrast. DAPI staining of the nucleus and kinetoplast is shown in blue. Scale bar represents 5 μm

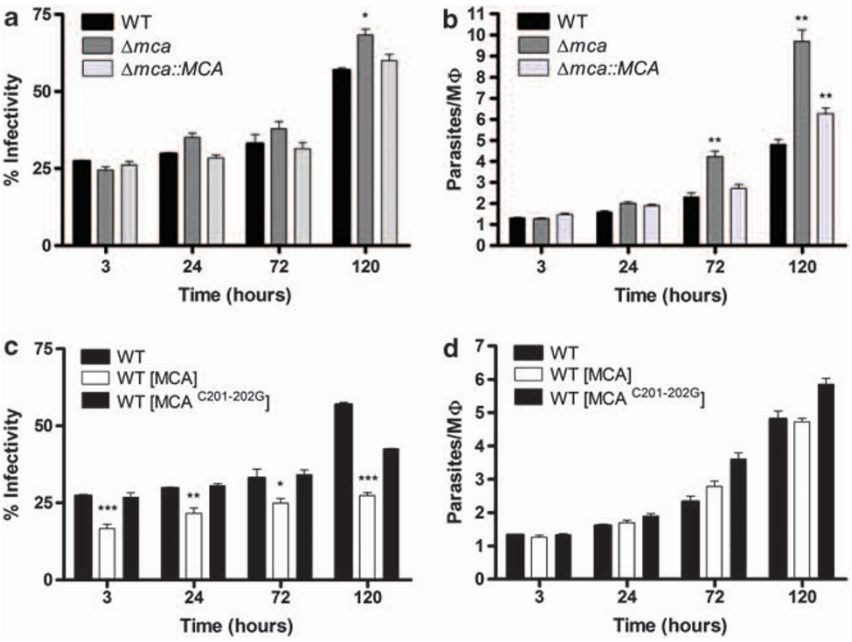

Figure 3 *In vitro* macrophage infectivity assay with promastigotes. PEMs were infected with *L. mexicana* stationary-phase promastigotes at a ratio of five promastigotes to one PEM for 3 h at 32°C and 5% CO_2. The parasite load was determined by counting the number of infected PEMs (**a** and **c**) and the number of intracellular parasites (**b** and **d**) after 3, 24, 72 and 120 h of incubation. Data show the percentage of infected macrophages and the number of parasites per macrophage (means ± s.d from four points) of a representative experiment out of three independent infections. Significant differences compared with WT are indicated as follows (*t*-test, ***$P<0.001$; **$P<0.01$; and *$P<0.05$)

with WT (MCA) was significantly lower than with WT (Figure 3c), although intracellular multiplication was similar (Figure 3d). The infectivity of WT ($MCA^{C201-202G}$) was not significantly different from WT, indicating that the lower infectivity phenotype of WT (MCA) is dependent on the proteolytic activity of MCAs.

We extended our study using amastigotes isolated from animal lesions. The results are consistent with those using promastigotes, but the differences between the mutants and WT were more pronounced with greater differences being found at more time points (Figures 4a and b). In addition, WT (MCA) multiplied more slowly within PEMs than did WT (Figure 4b). To further corroborate the findings, we also used axenic amastigotes that had been differentiated from promastigotes *in vitro*, which yielded results very similar to those with lesion-derived amastigotes (Figures 4c and d).

The ability of the different lines to produce lesions in mice was also investigated. Stationary-phase promastigotes (2×10^6) were injected into the footpad of BALB/c mice and lesion development monitored. Footpad measurements indicated that Δ*mca* formed significantly larger lesions than WT and Δ*mca*::*MCA* parasites over an 8-week period (Figure 5a), whereasWT (MCA) parasites formed significantly smaller lesions than WT or WT ($MCA^{C201-202G}$) (Figure 5b). These data show that *L. mexicana* lacking MCAs are more virulent than WT in macrophages *in vitro* and in mice *in vivo* and that overexpression of MCAs has the opposite effect of reducing parasite growth, the latter phenotype being dependent on the expression of an active MCA.

Analysis of *MCA*-deficient mutants. It has been reported that overexpression of *Leishmania* MCAs enhances sensitivity to inducers of cell death,[28,29] including heat shock,[8,12] hydrogen peroxide,[6] ROS[7] and drugs such as MLF and CPT.[9,10] Thus, we tested whether *L. mexicana* Δ*mca* would be protected against cell death induced by some of these agents. A method commonly used to assess cell death in *Leishmania* is propidium iodide (PI) staining, which has been applied to detect cells undergoing necrosis. In addition, annexin V (Ann V) labelling, which has been used extensively as a cell death marker in *Leishmania*,[8,31,32] is presumed to bind PS. Promastigotes were cultured in the presence of 20 μM MLF for 15 h whereupon PI staining and Ann V labelling was assessed. In all, 96% of WT and Δ*mca* promastigotes were Ann V^- PI^- under normal growth conditions, whereas after treatment with MLF only 37% of WT promastigotes remained Ann V^- PI^-. In total, 72% of MLF-treated Δ*mca* were Ann V^- PI^-, showing that Δ*mca* were less susceptible to MLF-induced cell death (Figure 6a). Recently it has been reported that *Leishmania* promastigotes have very low levels of PS,[33] so Ann V may not be a particularly suitable marker for regulated cell death in this parasite. However, the differences in Ann V labelling detected between WT and Δ*mca* parasites treated with MLF suggests that biochemical changes have occurred to the surface of the parasites and these are worthy of further investigation. Δ*mca* had a higher IC_{50} for MLF than WT, a difference reversed by re-expression of MCAs (Figure 6b). Importantly, however, Δ*mca* were not similarly less susceptible than WT to other stimuli reported to trigger cell death in

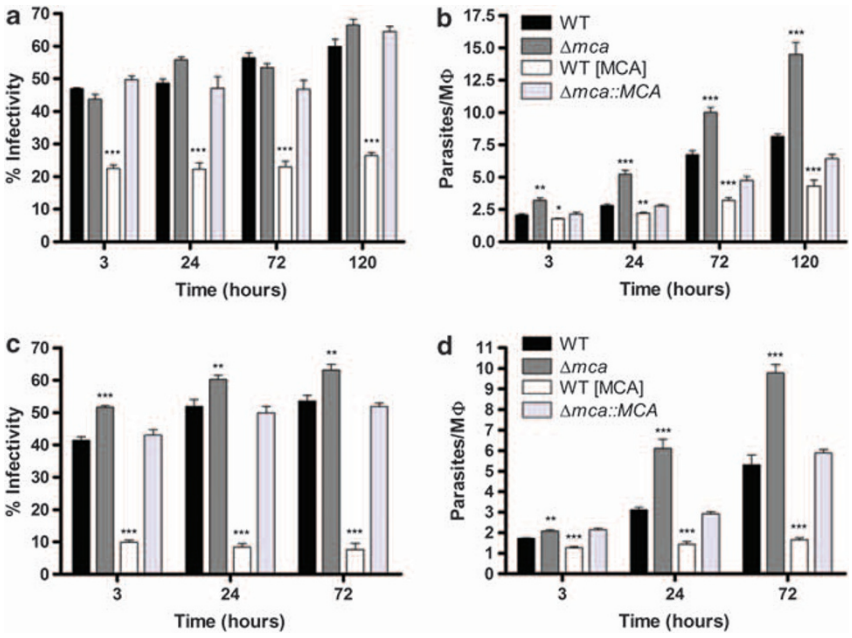

Figure 4 *In vitro* macrophage infectivity assay with amastigotes. PEMs were infected with *L. mexicana* amastigotes from lesions (**a**, **b**) or axenic amastigotes, (**c**, **d**) at 2 : 1 or 1 : 1 ratio, respectively, for 3 h. The percentage of infected PEMs (**a** and **c**) and the number of amastigotes per PEMs (**b** and **d**) were determined after 3, 24, 72 and 120 h of incubation. Data show the percentage of infected macrophages and the number of parasites per macrophage (means ± s.d from four points) of a representative experiment out of three independent infections. Significant differences compared with WT are indicated as follows (*t*-test, ***$P<0.001$; **$P<0.01$; and *$P<0.05$)

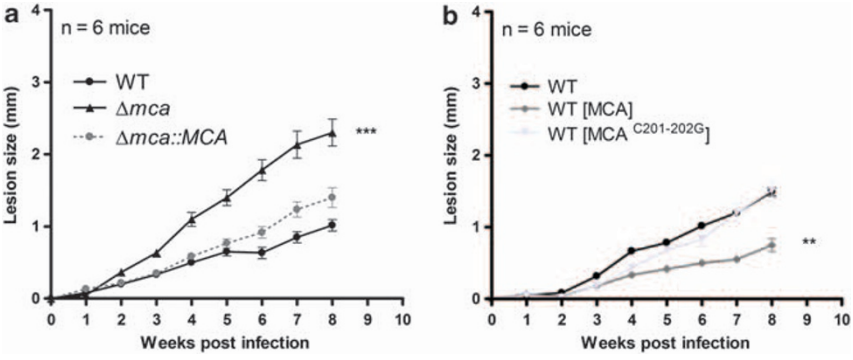

Figure 5 Infectivity to mice. (**a** and **b**) Infection of BALB/c mice with stationary-phase *L. mexicana* promastigotes. Groups of mice ($n=6$) were infected with 2×10^6 parasites in the right footpad. The ability of the different cell lines to produce lesions in mice was monitored using a calliper. Data shown represent the mean lesion size ± s.d from groups of six mice. Significant differences are indicated are indicated as follows (*t*-test, ***$P<0.001$; **$P<0.01$)

Leishmania, such as oxidative stress (data not shown) or CPT (Figure 6b).

To determine the ability of Δ*mca* amastigotes to persist within macrophages in the presence of MLF, PEMs were infected with WT and Δ*mca* promastigotes for 24 h and then treated with 30 μM MLF. The percentage of infected macrophages and the number of amastigotes per macrophage were determined after 3 days of drug treatment. The infectivity and number of amastigotes of Δ*mca* per macrophage was significantly higher than WT (Supplementary Figures S1A and B) under the same conditions. This suggests that Δ*mca* parasites replicate better in macrophages, even in the presence of MLF. To investigate the susceptibility of Δ*mca* amastigotes to killing by macrophages, PEMs were infected with WT and Δ*mca* promastigotes for 3 h and subsequently stimulated with LPS and IFN-γ (Supplementary Figures S1C and D). Δ*mca* were found to be significantly more resistant to killing by activated macrophages compared with WT.

It has been reported that MLF causes *L. donovani* promastigote cell death through mitochondrial dysfunction[11] and that overexpression of MCAs in *L. major* resulted in impaired mitochondrial membrane potential,[28] thus we reasoned that lack of MCAs may also affect the mitochondrion. Our results show that the mitochondrial membrane potential of Δ*mca* promastigotes was 36% that of WT, whereas overexpression of MCAs had a smaller effect with the mitochondrial membrane potential of WT (MCA) being 87% of WT (Figure 6c). In spite of the reduced mitochondrial membrane potential of Δ*mca* promastigotes, they were viable, grew at rates comparable to those of WT (Figure 1e) and had

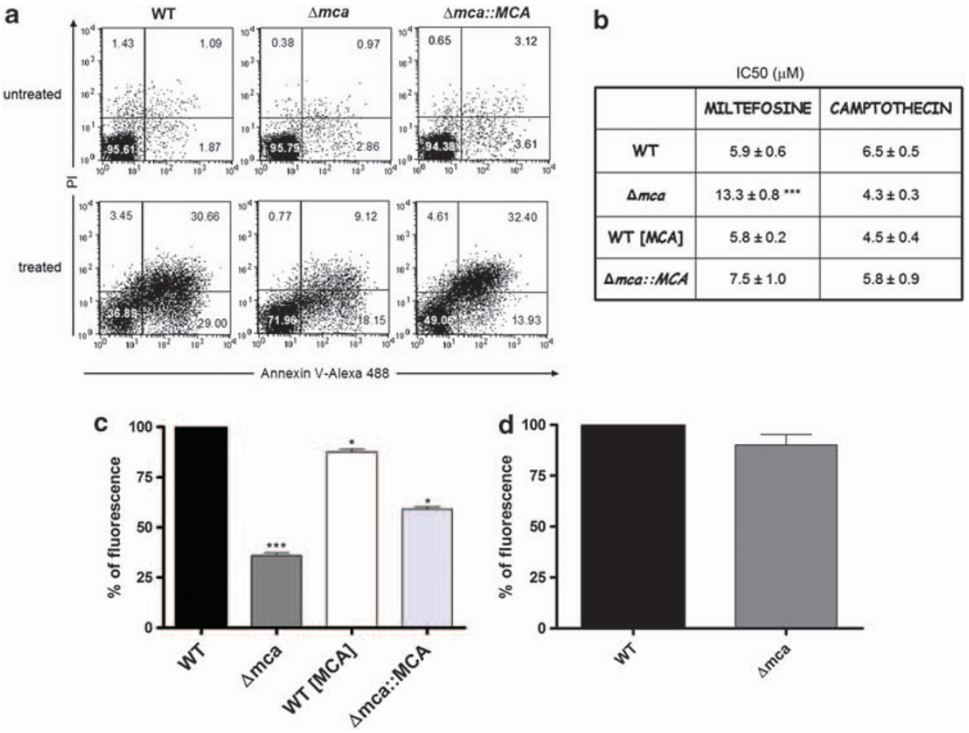

Figure 6 Drug-induced cell death and the mitochondrion. (**a**) Ann V labelling of MLF-treated parasites. Promastigotes were incubated with 20 μM MLF for 15 h, co-stained with Annexin-V Alexa 488 and analysed by flow cytometry. Numbers represent the percentage of cells in each of the quadrants. Dot plots are representative of three independent assays. (**b**) Leishmanicidal activity of MLF and CPT. Cell viability of *L. mexicana* promastigotes incubated with increasing concentrations of drugs was determined using a 3-(4,5-dimethylthiazol-2-yl)-2,5-diphenyl tetrasodium bromide assay. Results are expressed as the drug concentration (μM) necessary to inhibit parasite growth by 50% (IC_{50}). Results are the mean ± s.d of six independent experiments. Significant differences compared with WT were determined by the Student's *t*-test (***$P<0.001$). Determination of mitochondrial membrane potential using TMRM. *L. mexicana* promastigotes (**c**) or axenic amastigotes (**d**) were incubated with TMRM and analysed by flow cytometry to measure mitochondrial membrane potential. Data are shown as the percentage of mitochondrial membrane potential compared with WT; a representative graph out of three independent experiments is shown. *** and * significant differences compared with WT (*t*-test, ***$P<0.001$, *$P<0.05$)

an intact mitochondrion as assessed by tetramethylrhodamine methyl ester perchlorate (TMRM) labelling (data not shown). When the mitochondrial membrane potential of Δ*mca* axenic amastigotes was investigated, no significant differences compared with WT were found (Figure 6d).

Previous studies have reported a role for yeast MCA in clearance of insoluble aggregates,[25] but we could not detect any alteration in autophagy in Δ*mca* promastigotes (Supplementary Figure S2), suggesting that MCAs do not have a role in clearance of protein aggregates via autophagy or in the induction of autophagic cell death. TSN was identified as a common substrate for both Norway spruce MCA and human caspase-3,[22] but our studies indicate that TSN is not a substrate for *L. mexicana* MCA (Supplementary Figure S3). It is well established that *Leishmania* releases virulence factors that promote parasite survival in macrophages,[4,34] so we tested whether *L. mexicana* MCA is secreted and thereby modulates functions of the host cell to promote *Leishmania* replication. No release of MCAs was detected (Supplementary Figure S4).

Discussion

We demonstrate in this study that *MCAs* can be successfully deleted from *L. mexicana* promastigotes, generating viable null mutants. We attribute this achievement, in contrast to our previous report on genetic manipulation of *L. major* MCA,[27] to the use of a relatively new transfection method, the Nucleofector, which provides high transformation efficiency while being protective of cellular function. Indeed, we have now used the same methods to generate *L. major* MCA null mutants (data not shown), showing that there is not a noteworthy difference in the requirement for MCAs in the two species. The absence of MCA in *L. mexicana* did not produce an observable procyclic promastigote cell growth phenotype, as cells were viable and grew at a rate comparable to WT. Δ*mca* parasites also differentiated to amastigotes, both axenically *in vitro* and in macrophages, showing that absence of MCA did not prevent life cycle progression.

The most striking phenotype noted for the Δ*mca* parasites was their replication as amastigotes. The proliferation of Δ*mca* amastigotes in macrophages was significantly higher than WT and this was also the case in mice (Figures 3 and 4). This growth regulation was not apparent in axenic amastigotes (Figure 1f), possibly a reflection of the growth rate in axenic culture (doubling time of ~23 h) being significantly higher than in macrophages *in vitro* (doubling time of ~90 h) or in mice. As a corollary, overexpression of MCAs in amastigotes resulted in a lower replication rate compared with WT, both in macrophages and in mice, and this

phenotype was dependent on the proteolytic activity of MCAs. This suggests that MCAs act as an amastigote-specific growth suppressor, having a role in regulation of proliferation in the mammalian host. MCA in *L. mexicana* was shown to be located in small punctate structures in the cytoplasm of the parasite (Figure 2), which is a similar location to that determined for MCA in *L. major*.[27,28] The *L. major* enzyme was also found in the mitochondrion[27,28] and associated with the mitotic spindle,[27] whereas the *L. donovani* MCA has been reported to reside in acidocalcisomes[29] – a location we do not observe in *L. mexicana*. It is plausible that different processed forms of MCAs[28] are targeted to distinct subcellular compartments and that the isoform with an intact C-terminal domain is associated with the punctate structures. The finding that MCA is not released by either promastigotes or amastigotes (Supplementary Figure S4) correlates with this localisation data as well as a previous proteomic analysis of the *Leishmania* secretome that did not detect released MCAs,[35] suggesting that MCAs either acts directly within *Leishmania* to influence amastigote growth or that it processes a secreted protein that influences macrophage function to promote the rate of parasite proliferation. Two *Leishmania* peptidases CBP and GP63 are known to be released into the macrophage, where they modulate host cell signalling and promote parasite survival,[34,36–38] but these peptidases are thought to be activated by autocatalytic cleavage of an inhibitory pro-domain during intracellular trafficking[39,40] rather than as part of a proteolytic activation cascade. It is known that the MCA MCA3 of *T. brucei* processes MCA4, a catalytically inactive pseudopeptidase that acts as a virulence factor through modulation of parasite growth in the mammalian host.[41] However, MCA pseudopeptidases are apparently absent from the *L. mexicana* genome[42] and so different growth regulation mechanisms must exist in these trypanosomatids.

We proposed previously that stress-induced cell death of *Leishmania* might be mediated by the release of lysosomal enzymes after organelle disruption and that this could involve cleavage of MCAs by the released cathepsin-like cysteine peptidases.[12] Support for this hypothesis arose from the finding that a significant level of MCA processing was observed after H_2O_2 treatment in *L. major* overexpressing MCAs.[28] Such processing of *L. major* MCA influences its subcellular location, as the enzyme encodes a mitochondrial localisation domain and a cytosolic retention domain that together modulate the balance of MCAs between the mitochondrial and cytosolic compartments.[28] In this study, we have also observed a significant level of processing of *L. mexicana* MCAs in the overexpressor cell line (Figure 1d), which exhibits reduced cell proliferation as axenic amastigotes, as intracellular amastigotes and in mice (Figures 1f, 3c and 5d). The enzymatic activity of MCAs was crucial for the observed growth defects, as mutation of the two cysteine residues in the active site of MCAs, and which are crucial for enzymatic activity,[19,27] resulted in cells with WT proliferation rates. A significant level of processing was also observed in the WT ($MCA^{C201-202G}$) cell line (Figure 1d), which was not observed in a Δ*mca* ($MCA^{C201-202G}$) cell line (data not shown), suggesting that intermolecular cleavage by MCAs was occurring in WT ($MCA^{C201-202G}$). Overexpression of MCAs in WT parasites also enhanced sensitivity to H_2O_2-induced cell death in both *L. major*[28] and *L. donovani*,[29] most likely through impairment of mitochondrial function.[28] Our results with *L. mexicana* Δ*mca*, however, show that even though the MCA-deficient mutant has reduced mitochondrial membrane potential, as assessed with TMRM (Figure 6c), it is not more or less susceptible to cell death inducers such as H_2O_2 than WT *L. mexicana*. Thus, clearly *Leishmania* MCA is not essential for cell death processes even though cell death is exacerbated when MCA is overexpressed.[28,29] This MCA effect could occur through disruption of the distribution of MCAs between the cytosol and mitochondrion due to uncontrolled cleavage of MCAs by the cathepsin-like cysteine peptidases released from the lysosome, or through inappropriate activation of the enzyme in either compartment, which results in cleavage of non-physiological substrates.

In conclusion, we provide evidence that MCA is not essential for *Leishmania* proliferation, and our data provide no support for the proposed role of MCAs in regulated cell death. Rather our results suggest that MCA acts as an amastigote-specific growth suppressor, thereby regulating proliferation of the parasite in the mammalian host. Such self-regulation of growth is likely to be crucial in the maintenance of the intensity of infection in the mammalian host and thus be contributing greatly to pathogenesis.

Materials and Methods

Parasites. *L. mexicana* (MNYC/BZ/62/M379) promastigotes were grown in HOMEM medium with 10% (v/v) heat-inactivated foetal calf serum (FCS) at 25°C as described previously.[43] *In vitro* culture of *L. mexicana* axenic amastigotes was performed in Schneider's *Drosophila* medium supplemented with 20% (v/v) FCS, pH 5.0, at 32°C in 5% CO_2 as described previously.[44]

Generation of *L. mexicana* transgenic cell lines. For targeted gene replacement of the *L. mexicana MCA* gene (LmxM.34.1580), the 452-bp DNA fragment comprising the 5′ flanking region plus 5′ end of *MCA* was amplified by PCR from *L. mexicana* genomic DNA using the primer pair OL3099 (*Hin*dIII) and OL3092 (*Sal*I; all oligonucleotides used in this study can be found in Supplementary Table S1). The 3′ flanking region of *MCA* was generated by PCR using the primer pair OL3020 (*Xma*I) and OL3021 (*Bgl*II). Using *Hin*dIII/*Sal*I and *Xma*I/*Bgl*II digestion, the 5′ and 3′ flanks were sequentially ligated into pGL345, to yield the hygromycin-resistant construct pGL1922. The bleomycin-resistant plasmid pGL1923 was generated from pGL1922, replacing the *HYG* cassette by *Spe*I/*Bam*HI digest. Clones of parasites resistant to hygromycin were generated after transfection with *Hin*dIII/*Bgl*II-linearised pGL1922, and a second round of transfection with linearised pGL1923 generated hygromycing–bleomycin double-resistant clones. The absence of MCA was assessed by both PCR and Southern blot.

For the re-integration construct, *MCA* was amplified with OL3420 and OL3421 primers, subcloned in pGEM-T easy vector and, following digestion with *Xho*I/*Bam*HI, ligated in *Xho*I/*Bgl*II-digested pGL631 (pRIB)[45] to generate the re-expressor construct pGL2004. The integration cassette was obtained by digestion with *Pac*I/*Pme*I before transfection, and clones were selected for puromycin resistance.

For episomal expression, *MCA* from *L. mexicana* was isolated from genomic DNA using OL3399 and OL3400 primers. The 1320-bp fragment was subcloned into *Xba*I/*Xho*I-digested pTEX vector to generate pGL1984. To obtain parasites overexpressing the active site mutant MCA ($MCA^{C201-202G}$), the two cysteines in the catalytic site were mutated by site-directed mutagenesis using OL1841 and OL1842 primers, to produce the active site mutant construct pGL2022. Site-directed mutagenesis was performed using the QuickChange mutagenesis kit (Stratagene, La Jolla, CA, USA) according to the manufacturer's instruction, and confirmed by DNA sequencing.

Transfection procedure. Mid-log phase *L. mexicana* promastigotes were transfected with 10 μg of plasmid or digested DNA by electroporation using the Nucleofector system with the Human T-Cell Nucleofector kit (Lonza, Basel, Switzerland). Briefly, 5×10^7 log-phase cells were harvested by centrifugation at

1000 × *g* for 10 min. The cell pellet was resuspended in 100 μl of Human T Cell Nucleofector Solution, transferred to Amaxa electroporation cuvettes and mixed with 10 μg of DNA. Cells were nucleoporated on program U-033 on the Nucleofector machine (Amaxa GmbH, Cologne, Germany). Following electroporation, cells were incubated in their culture medium overnight and transfectants were cloned by limiting dilution with the appropriate antibiotics: 50 μg/ml hygromycin B (Invitrogen, Paisley, UK), 50 μg/ml G418 (Calbiochem, Nottingham, UK), 10 μg/ml phleomybin (InvivoGen, San Diego, CA, USA), 50 μg/ml puromycin (Calbiochem).

Southern blot analysis. Genomic DNA of *L. mexicana* WT, heterozygotes and null mutants (Δ*mca*) was purified using the de DNAeasy kit (Qiagen, Crawley, UK), digested with *Age*I/*Sac*II and transferred to Hybond-N membranes (GE Healthcare, Little Chalfont, UK) following standard procedures and as described previously.[43] Blots were hybridised with an alkaline-phosphatase-labelled DNA probe (AlkPhos Direct labelling, GE Healthcare) comprising the 5′ flanking region used for targeted gene replacement, or 500 bp of the *MCA* ORF.

Immunoblotting. For western blot analysis, 1.5×10^7 cells were loaded per lane of a 10% NuPAGE Bis-Tris gel (Invitrogen) in MOPS running buffer and transferred onto Hybond-C nitrocellulose membranes (GE Healthcare). Primary antibodies against LmjMCA,[27] HA (Roche, Mannheim, Germany), EF1-α (Millipore, Bedford, MA, USA) and BiP (gift from JD Bangs (University of Wisconsin, Madison, WI, USA)) were used at 1 : 100, 1 : 1000, 1 : 10 000 and 1 : 10 000, respectively. Horseradish peroxidase-conjugated anti-rabbit (Promega, Southampton, UK) was used at 1 : 5000, anti-rat (Millipore) and anti-mouse (Promega) were used at 1 : 10 000. Chemiluminescence was detected using ECL plus (GE Healthcare) or Novex ECL (Invitrogen).

Immunoflurescence. Parasites were fixed in 1% formaldehyde, permeabilised with 0.1% Triton and neutralised with 0.1 M glycine. Cells were attached to poly-lysine-treated slides and blocked with TB buffer (PBS with 0.1% Triton and 0.1% BSA). A 1 : 100 dilution of α-LmjMCA antibody in TB buffer was applied for 1 h at room temperature. After washing the slides three times with PBS, anti-rabbit Alexa Fluor 594-conjugated antibody (Molecular probes, Eugene, OR, USA) at 1 : 2000 in TB buffer was added and the slides were incubated for 1 h in the dark at room temperature. Cellular DNA was stained with 1 μg/ml DAPI in TB buffer. A mounting solution (2.5% 1,4-diazabicyclo(2.2.2)octane in 50% glycerol) was then applied to the slides. Images were obtained using an Applied Precision DeltaVision Deconvolution microscope system (Applied Precision, Inc. Issaquah, WA, USA) fitted with a Photometrics CoolSnap HQ (Roper Scientific, Inc. Tucson, AZ, USA) camera. Fluorescence images were acquired with the RDTRPF filter (λ_{Ex} 555 nm/λ_{Em} 617 nm) and DAPI filter (λ_{Ex} 360 nm/λ_{Em} 457 nm). References images were obtained with the differential interference contrast filter.

Induction of cell death. Drug-induced cell death was attempted by incubating the parasites in the presence of 20 μM MLF for 15 h. For Ann V labelling 1.5×10^6 treated cells were washed with Ann V buffer (20 mM HEPES; 132 mM NaCl; 3.5 mM KCl; 0.5 mM $MgCl_2$; pH 7.3, supplemented with 10 mM glucose and 5 mM $CaCl_2$) and incubated with Ann V-alexa 488 (Molecular Probes) for 15 min in the dark. Propidium iodine 0.4 μg/ml was added for 5 min. Cold PBS was added to the samples, which were analysed in a BD FACScalibur (BD Biosciences, San Jose, CA, USA) equipped with an FL1 (530/30 nm) and FL2 (585/42 nm) filter. Drug sensitivities of promastigotes were determined using a 3-(4,5-dimethylthiazol-2-yl)-2,5-diphenyl tetrasodium bromide-based assay as described previously.[46] IC_{50} was the drug concentration required for half-maximal inhibition of the cellular growth rate.

Measurement of mitochondrial membrane potential. Log-phase promastigotes or axenic amastigotes were incubated with 50 nM TMRM (Sigma, Gillingham, UK) for 30 min and analysed by flow cytometry. Fluorescence was detected in FL2. The experiment was performed in triplicate, normalised to 100% of WT.

Macrophage infectivity assay. PEMs were extracted from peritoneal lavage of female ICR mice. Cells were plated in Lab-teck 16-well chamber slides (VWR International Ltd, East Grinstead, West Sussex, UK) at a density of 5×10^4 cells/well and incubated overnight at 37°C and 5% $C0_2$ in RPMI supplemented with 10% FCS. Cells were incubated with stationary-phase promastigotes at 5 : 1 promastigotes: macrophage ratio for 3 h at 32°C and 5% $C0_2$, after which they were washed to remove extracellular parasites and were incubated for 24, 72 or 120 h to allow intracellular replication. Cells were fixed for 20 min at 4°C with 2% formaldehyde following permeabilisation with 0.1% Triton X-100 for 10 min and stained with Vectashield mounting media with DAPI (Vector Laboratories, Burlingame, CA, USA) to identify the parasites. The percentage of infected macrophages and number of amastigotes per infected macrophage were determined by examination of 200 macrophages per well, in quadruplicates, under fluorescence microscopy using a Zeiss Axioskop 2 (Zeiss Ltd, Cambridge, UK) fluorescence microscope.

Lesion-derived amastigotes were obtained from infected BALB/c mice, removing the footpad and rupturing it to homogeneity with the back of a syringe through a nylon membrane in RPMI supplemented with 10% FCS as described previously.[44] Lesion-derived amastigotes or axenic amastigotes were used to infect macrophages at a 2 : 1 ratio or 1 : 1, respectively, for 3 h. Extracellular parasites were removed by washing, and fresh medium was added. Cultures were maintained at 32°C and 5% $C0_2$ for 24, 72 or 120 h, after which cells were fixed and stained as stated above. For testing amastigote sensitivity to MLF, peritoneal macrophages were infected with stationary-phase promastigotes at a 5 : 1 ratio for 24 h. Extracellular parasites were removed by washing and fresh medium containing 30 μM MLF was added. Cells were maintained at 32°C and 5% CO_2 for 24, 72 or 120 h, after which cells were fixed, stained and counted as stated above.

Infection of mice. Groups of six female BALB/c mice were inoculated in the right footpad with 2×10^6 stationary-phase *L. mexicana* promastigotes in PBS. Lesion development was monitored weekly over an 8–12-week period, until the footpad reached a thickness of 5 mm, when mice were culled.

Statistical analysis. All data were analysed by the Student's *t*-test. The GraphPad Instat software (San Diego, CA, USA) was used to perform the analysis. Differences were considered significant when $P<0.05$. Significant differences are indicated as follows: $^{***}P<0.001$, $^{**}P<0.01$ and $^{*}P<0.05$.

Additional Materials and Methods can be found in Supplementary Information.

Conflict of Interest

The authors declare no conflict of interest.

Acknowledgements. We thank William Proto for his helpful comments on the manuscript. This work was supported by the Medical Research Council (grant number 0700127). The Wellcome Trust Centre for Molecular Parasitology is supported by core funding from the Wellcome Trust (085349).

1. Taylor RC, Cullen SP, Martin SJ. Apoptosis: controlled demolition at the cellular level. *Nat Rev Mol Cell Biol* 2008; **9**: 231–241.
2. Debrabant A, Lee N, Bertholet S, Duncan R, Nakhasi HL. Programmed cell death in trypanosomatids and other unicellular organisms. *Int J Parasitol* 2003; **33**: 257–267.
3. Murray HW, Berman JD, Davies CR, Saravia NG. Advances in leishmaniasis. *Lancet* 2005; **366**: 1561–1577.
4. Kaye P, Scott P. Leishmaniasis: complexity at the host – pathogen interface. *Nat Rev Micro* 2011; **9**: 604–615.
5. Lee N, Bertholet S, Debrabant A, Muller J, Duncan R, Nakhasi HL. Programmed cell death in the unicellular protozoan parasite *Leishmania*. *Cell Death Differ* 2002; **9**: 53–64.
6. Das M, Mukherjee SB, Shaha C. Hydrogen peroxide induces apoptosis-like death in *Leishmania donovani* promastigotes. *J Cell Sci* 2001; **114**: 2461–2469.
7. Holzmuller P, Sereno D, Cavaleyra M, Mangot I, Daulouede S, Vincendeau P *et al.* Nitric oxide-mediated proteasome-dependent oligonucleosomal DNA fragmentation in *Leishmania amazonensis* amastigotes. *Infect Immun* 2002; **70**: 3727–3735.
8. Moreira MEC, Del Portillo HA, Milder RV, Balanco JMF, Barcinski MA. Heat shock induction of apoptosis in promastigotes of the unicellular organism *Leishmania (Leishmania) amazonensis*. *J Cell Physiol* 1996; **167**: 305–313.
9. Paris C, Loiseau PM, Bories C, Breard J. Miltefosine induces apoptosis-like death in *Leishmania donovani* promastigotes. *Antimicrob Agents Chemother* 2004; **48**: 852–859.
10. Sen N, Das BB, Ganguly A, Mukherjee T, Tripathi G, Bandyopadhyay S *et al.* Camptothecin induced mitochondrial dysfunction leading to programmed cell death in unicellular hemoflagellate *Leishmania donovani*. *Cell Death Differ* 2004; **11**: 924–936.
11. Verma NK, Singh G, Dey CS. Miltefosine induces apoptosis in arsenite-resistant *Leishmania donovani* promastigotes through mitochondrial dysfunction. *Exp Parasitol* 2007; **116**: 1–13.

12. Zangger H, Mottram JC, Fasel N. Cell death in *Leishmania* induced by stress and differentiation: Programmed cell death or necrosis? *Cell Death Differ* 2002; **9**: 1126–1139.
13. Reece SE, Pollitt LC, Colegrave N, Gardner A. The meaning of death: Evolution and ecology of apoptosis in protozoan parasites. *PLoS Pathog* 2011; **7**: e1002320.
14. Ivens AC, Peacock CS, Worthey EA, Murphy L, Aggarwal G, Berriman M *et al.* The genome of the kinetoplastid parasite, *Leishmania major*. *Science* 2005; **309**: 436–442.
15. Berriman M, Ghedin E, Hertz-Fowler C, Blandin G, Renauld H, Bartholomeu DC *et al.* The genome of the African trypanosome *Trypanosoma brucei*. *Science* 2005; **309**: 416–422.
16. Uren GA, O'Rourke K, Aravind L, Pisabarro TM, Seshagiri S, Koonin VE *et al.* Identification of paracaspases and metacaspases: two ancient families of caspase-like proteins, one of which plays a key role in MALT lymphoma. *Mol Cell* 2000; **6**: 961–967.
17. Vercammen D, van de Cotte B, De Jaeger G, Eeckhout D, Casteels P, Vandepoele K *et al.* Type II metacaspases Atmc4 and Atmc9 of *Arabidopsis thaliana* cleave substrates after arginine and lysine. *J Biol Chem* 2004; **279**: 45329–45336.
18. Moss CX, Westrop GD, Juliano L, Coombs GH, Mottram JC. Metacaspase 2 of *Trypanosoma brucei* is a calcium-dependent cysteine peptidase active without processing. *FEBS Lett* 2007; **581**: 5635–5639.
19. Gonzales IJ, Desponds C, Schaff C, Mottram JC, Fasel N. *Leishmania major* metacaspase can replace yeast metacaspase in programmed cell death and has arginine-specific cysteine peptidase activity. *Int J Parasitol* 2007; **37**: 161–172.
20. Bozhkov PV, Suarez MF, Filonova LH, Daniel G, Zamyatnin AA Jr, Rodriguez-Nieto S *et al.* Cysteine protease mcII-Pa executes programmed cell death during plant embryogenesis. *PNAS* 2005; **102**: 14463–14468.
21. McLuskey K, Rudolf J, Proto WR, Isaacs NW, Coombs GH, Moss CX *et al.* Crystal structure of a *Trypanosoma brucei* metacaspase. *Proc Natl Acad Sci USA* 2012; **109**: 7469–7474.
22. Sundstrom JF, Vaculova A, Smertenko AP, Savenkov EI, Golovko A, Minina E *et al.* Tudor staphylococcal nuclease is an evolutionarily conserved component of the programmed cell death degradome. *Nat Cell Biol* 2009; **11**: 1347–1354.
23. Tsiatsiani L, Van BF, Gallois P, Zavialov A, Lam E, Bozhkov PV. Metacaspases. *Cell Death Differ* 2011; **18**: 1279–1288.
24. Lee RE, Puente LG, Kaern M, Megeney LA. A non-death role of the yeast metacaspase: Yca1p alters cell cycle dynamics. *PLoS ONE* 2008; **3**: e2956.
25. Lee RE, Brunette S, Puente LG, Megeney LA. Metacaspase Yca1 is required for clearance of insoluble protein aggregates. *Proc Natl Acad Sci USA* 2010; **107**: 13348–13353.
26. Coll NS, Vercammen D, Smidler A, Clover C, Van BF, Dangl JL *et al. Arabidopsis* type I metacaspases control cell death. *Science* 2010; **330**: 1393–1397.
27. Ambit A, Fasel N, Coombs GH, Mottram JC. An essential role for the *Leishmania major* metacaspase in cell cycle progression. *Cell death Diff* 2008; **15**: 113–122.
28. Zalila H, Gonzalez IJ, El-Fadili AK, Delgado MB, Desponds C, Schaff C *et al.* Processing of metacaspase into a cytoplasmic catalytic domain mediating cell death in *Leishmania major*. *Mol Microbiol* 2011; **79**: 222–239.
29. Lee N, Gannavaram S, Selvapandiyan A, Debrabant A. Characterization of metacaspases with trypsin-like activity and their putative role in programmed cell death in the protozoan parasite *Leishmania*. *Eukaryot Cell* 2007; **6**: 1745–1757.
30. Raina P, Kaur S. Knockdown of LdMC1 and Hsp70 by antisense oligonucleotides causes cell-cycle defects and programmed cell death in *Leishmania donovani*. *Mol Cell Biochem* 2012; **359**: 135–149.
31. van Zandbergen G, Bollinger A, Wenzel A, Kamhawi S, Voll R, Klinger M *et al. Leishmania* disease development depends on the presence of apoptotic promastigotes in the virulent inoculum. *PNAS* 2006; **103**: 13837–13842.
32. van Zandbergen G, Luder CG, Heussler V, Duszenko M. Programmed cell death in unicellular parasites: a prerequisite for sustained infection? *Trends Parasitol* 2010; **26**: 477–483.
33. Williams RAM, Smith TK, Cull B, Mottram JC, Coombs GH. ATG5 is essential for ATG8-dependent autophagy and mitochondrial homeostasis in *Leishmania*. *PLoS Path* 2012; **8**: e1002695.
34. Jaramillo M, Gomez M-A, Larsson O, Shio M-T, Topisirovic I, Contreras I *et al. Leishmania* repression of host translation through mTOR cleavage is required for parasite survival and infection. *Cell Host Microbe* 2011; **9**: 331–341.
35. Silverman JM, Chan SK, Robinson DP, Dwyer DM, Nandan D, Foster LJ *et al.* Proteomic analysis of the secretome of *Leishmania donovani*. *Genome Biol* 2008; **9**: R35.
36. Cameron P, McGachy A, Anderson M, Paul A, Coombs GH, Mottram JC *et al.* Inhibition of Lipopolysaccharide-induced macrophage IL-12 production by *Leishmania mexicana* amastigotes: the role of cysteine peptidases and the NF-κB signaling pathway. *J Immunol* 2004; **173**: 3297–3304.
37. Halle M, Gomez MA, Stuible M, Shimizu H, McMaster WR, Olivier M *et al.* The *Leishmania* surface protease GP63 cleaves multiple intracellular proteins and actively participates in p38 mitogen-activated protein kinase inactivation. *J Biol Chem* 2009; **284**: 6893–6908.
38. Contreras I, Gomez MA, Nguyen O, Shio MT, McMaster RW, Olivier M. *Leishmania*-induced inactivation of the macrophage transcription factor AP-1 is mediated by the parasite metalloprotease GP63. *PLoS Pathog* 2010; **6**: e1001148.
39. Brooks DR, Tetley L, Coombs GH, Mottram JC. Processing and trafficking of cysteine proteases in *Leishmania mexicana*. *J Cell Sci* 2000; **113**: 4035–4041.
40. Ellis M, Sharma DK, Hilley JD, Coombs GH, Mottram JC. Processing and trafficking of *Leishmania mexicana* GP63: analysis using mutants deficient in glycosylphosphatidyl inositol protein anchoring. *J Biol Chem* 2002; **277**: 27968–27974.
41. Proto WR, Castanys-Munoz E, Black A, Tetley L, Juliano L, Coombs GH *et al. Trypanosoma brucei* metacaspase 4 is a pseudopeptidase and a virulence factor. *J Biol Chem* 2011; **286**: 39914–39925.
42. Rogers MB, Hilley JD, Dickens NJ, Wilkes JM, Bates PA, Depledge DP *et al.* Chromosome and gene copy number variation allow major structural change between species and strains of *Leishmania*. *Genome Res* 2011; **21**: 2129–2142.
43. Brooks DR, Denise H, Westrop GD, Coombs GH, Mottram JC. The stage-regulated expression of *Leishmania mexicana* CPB cysteine proteases is mediated by an intercistronic sequence element. *J Biol Chem* 2001; **276**: 47081–47089.
44. Bates PA, Robertson CD, Tetley L, Coombs GH. Axenic cultivation and characterization of *Leishmania mexicana* amastigote-like forms. *Parasitology* 1992; **105**: 193–202.
45. Mißlitz A, Mottram JC, Overath P, Aebischer T. Targeted integration into a rRNA locus results in uniform and high level expression of transgenes in *Leishmania* amastigotes. *Mol Biochem Parasitol* 2000; **107**: 251–261.
46. Williams RAM, Tetley L, Mottram JC, Coombs GH. Cysteine peptidases CPA and CPB are vital for autophagy and differentiation in *Leishmania mexicana*. *Mol Microbiol* 2006; **61**: 655–674.

Supplementary information accompanies the paper on Cell Death and Disease website (http://www.nature.com/cddis)